# ITRAX: description and evaluation of a new multi-function X-ray core scanner

IAN W. CROUDACE[1], ANDERS RINDBY[2] & R. GUY ROTHWELL[1]
[1]*National Oceanography Centre, Empress Dock, Southampton SO14 3ZH, UK*
[2]*Cox Analytical Systems, Ostergardsgatan 7, SE-431 53 Molndal, Sweden*

**Abstract:** A new automated multi-function core scanning instrument, named ITRAX, has been developed that records optical, radiographic and elemental variations from sediment half cores up to 1.8 m long at a resolution as fine as 200 μm. An intense micro-X-ray beam focused through a flat capillary waveguide is used to irradiate samples to enable both X-radiography and X-ray fluorescence (XRF) analysis. Data are acquired incrementally by advancing a split core, via a programmable stepped motor drive, through the flat, rectangular-section X-ray beam. Traditional XRF determination of element composition in sediments provides high-quality data, but it takes a considerable time and normally consumes gram quantities of material that is often only available in limited quantities. The ITRAX core scanner non-destructively collects optical and X-radiographic images, and provides high-resolution elemental profiles that are invaluable for guiding sample selection for further (destructive) detailed sampling. This paper presents a description of the construction, characteristics and capabilities of the ITRAX system. High-resolution ITRAX data obtained from sediment cores are also presented and compared with results from traditional wavelength-dispersive XRF analysis at lower resolution. Finally, some recent technical developments linked to the second-generation ITRAX are presented.

Elemental and other sediment property variations along core profiles can be used to infer environmental, sedimentological and diagenetic changes, pollution inputs and to assist in correlation studies. Traditional methods of acquiring solid-phase geochemical data from sediment cores are time-consuming and involve incremental sampling to obtain gram quantities of material and further processing before analysis by techniques such as X-ray fluorescence (XRF) analysis. Conventional XRF analysis requires dried and ground sediment and two sample preparation methods are commonly used (Croudace & Williams-Thorpe 1988; Croudace & Gilligan 1990; Jenkins 1999). The fusion method produces a solid solution in the form of a glass bead by dissolving about 0.5 g of sample in a lithium borate flux for determination of major and the more abundant trace elements. The pelletization method utilizes at least 3 g of ground sample, pressed into a briquette at 15–20 tonnes, and allows major and trace elements to be determined. Notably, material from these XRF pellets may be re-used for other analyses or tests. In conventional XRF analysis grinding and pelletization of samples reduces mineral and particle-size effects and density variations while the fusion variant circumvents particle-size and mineralogical problems and reduces inter-element effects by dissolving the sample and providing a consistent matrix. The entire preparation and analytical process for a 1 m core subsampled at 1 cm increments would take up to 2 weeks.

Non-destructive scanners that incorporate XRF analysis provide useful, high-resolution geochemical records from terrestrial and marine sediment and drilled rock cores (e.g. Jansen *et al*. 1998; Rothwell *et al*. 2006; Thomson *et al*. 2006). Particle size, mineralogy and density effects will exist in cores, and direct analysis will lead to some degradation of data quality compared to the well-controlled approaches used in the conventional XRF analysis procedures above. Some of the new scanners do, however, allow relatively rapid and continuous analysis of split sediment cores to provide records of downcore geochemical and textural variations. At present these instruments generally serve the valuable role of providing initial detailed characterization of sediment cores. Sections of interest can then be analysed at higher accuracy (although generally at poorer spatial resolution) using well-established, variably destructive methods such as XRF analysis or inductively coupled plasma optical emission spectroscopy.

## The ITRAX core scanner

The ITRAX core scanner (Fig. 1) is unique among the current generation of core scanners

*From*: ROTHWELL, R.G. 2006. *New Techniques in Sediment Core Analysis*. Geological Society, London, Special Publications, **267**, 51–63. 0305-8719/06/$15.00 © The Geological Society of London 2006.

**Fig. 1.** Front view of the ITRAX core scanner with open hoods. Split core sections are moved incrementally from the left extension to the right extension during analysis.

in being designed to gather optical and micro-radiographic images and micro-X-ray fluorescence spectrometry (μXRF) elemental profiles for the same sediment core section. It can operate on split cores of sediment or rock with a maximum length of 1800 mm and a diameter ranging from a few cm up to 12 cm. The instrument consists of a central measuring tower incorporating an X-ray focusing unit and a range of sensors. These sensors include an optical-line camera, a laser topographic scanner, an X-ray line camera for measuring the transmitted X-rays and a high count-rate XRF detection system. Further information on the technology incorporated into the ITRAX scanner is available from the literature (Rindby *et al.* 1997; Vincze *et al.* 1998; Janssens *et al.* 2000; Streli *et al.* 2004; Tsuji *et al.* 2004). On either side of the tower are two fixed projections that are part of the motorized split-core transport bed. 'Flat-beam' scanning technology (Bergström *et al.* 2001) is used to provide highly resolved, two-dimensional radiographic images and profiles of XRF spectral data over the selected sample length. The system is fitted with numerous safety interlocks to ensure mechanical and radiological security.

## *Scanning procedure and control software*

The ITRAX scanner is controlled from a central computer that runs on a Windows XP platform. Users control the system through a graphical user interface called the Core Scanner Navigator where standard operation procedures can be implemented and monitored (Table 1). A second program, Q-Spec, interacts with this interface and is activated automatically during certain operations. Q-Spec is primarily concerned with the display and on-the-fly analysis of XRF spectral data, but it can also be used to refine the X-ray spectral analysis after core scanning on the instrument is complete.

The standard ITRAX procedure starts by loading a split sediment core onto a horizontal cradle with the core-top positioned to the right. Scanning is initiated from the software and follows a logical and guided sequence involving inputs: (i) to define the core length to be scanned; (ii) setting the excitation voltage and current to the X-ray tube; and (iii) initiating a surface topographic scan of the core. This topographic scan is made in relation to a horizontal reference plane and is used to ensure that any subsequent positioning of the XRF detector does not lead to a collision of the detector with the sediment surface and, importantly, that the detector–sample distance is monitored and remains constant. The scanning occurs by a regular left to right incremental movement of the core perpendicular to the long axis of the rectangular beam (Fig. 2). This initial scan takes approximately 5 min after which the core is automatically returned to its start position. The next procedure (iv) involves defining the likely elements in the sample from a periodic table as well as adjusting and refining the peak-fitting parameters using one or more representative parts of the core sample. This optimization takes place with the operator ensuring

**Table 1.** *Summary of typical ITRAX operator procedures*

| Operator task or input | Result |
|---|---|
| Load split sediment core on to horizontal sample cradle | Sample ready for scanning |
| Define kV and mA setting for 3 kW Mo X-ray tube | Excitation condition set |
| Define core dimension to be scanned | Dimensional limits set for scanning |
| Initiate surface scanning/photographic procedure (approximately 5 min) | Surface topography profile determined and digital photographic image of core captured |
| Enter the scan increment size and the dwell time for the radiographic scan | Radiographic parameters set ready for the radiographic scan |
| Establish XRF parameters and select the elements likely to be present | Elements selected and spectral-fitting parameters refined |
| Set reference response for the radiographic camera by automatically removing the core from the X-ray beam | Calibration of the X-ray line camera diode array |
| Enter dialogue menu where data file storage locations are named and the XRF count time defined | Automated process commences with the acquisition of an incremental (digital) radiographic scan. The core is then returned to zero ready for next stage |
| Instrument commences XRF analysis | Incremental XRF scans acquired and stored |

that the best peak-fitting functions are chosen. The next step (v) is to record a reference response for the X-radiographic detector by automatically driving the core out of the path of the X-ray beam. This step calibrates and normalizes the response of the X-ray line camera diode array and takes approximately 1 min after which the core is returned to its start position. The final step in the Navigator panel is (vi) to enter the Batch Analysis Mode where the user defines the core name, reviews instrument count times, dwell times and scan limits before starting the scan process. The first operation of the ensuing automated process is to acquire and construct the X-radiographic image, after which the core again returns to the start position and then begins the incremental acquisition of XRF elemental profiles. The XRF spectral data are all stored and can, if necessary, be re-processed and refined by the user after scanning is complete. Such re-analysis may be required if the user has neglected to include an element for output or if some further refinement to the background or peak-fitting process is deemed necessary. A straightforward facility exists for efficiently reprocessing a batch of spectra.

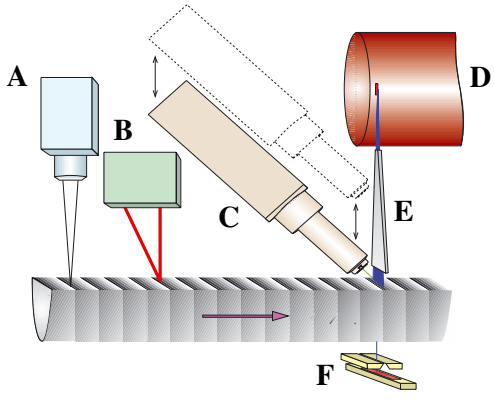


**Fig. 2.** Schematic of the ITRAX system showing the optical-line camera (A), laser triangulation system (B), motorized XRF Si-drift chamber detector (C), 3 kW X-ray tube (D), flat-beam X-ray waveguide (E) and the X-ray line camera and slit system for the radiographic line camera (F). The horizontal arrow shows the incremental motion direction of a core and the vertical arrows the movement directions of the XRF detector.

### *XRF spectral analysis software*

The Q-Spec spectral analysis software employs standard fitting procedures to extract the individual elemental peak areas from the spectrum. Each peak is described by a Gaussian function with an exponential tailing on the low-energy side with a step-like background function. The general spectral background is described with a multi-parameter function including polynomial as well as exponential terms. As previously mentioned, the operator selects from a periodic table the elements to be extracted from the X-ray spectra. Any incorrect or unnecessary elemental choices or incorrect fitting parameters can be adjusted later through a batch-controlled post-processing of the spectra.

## *Instrumental components*

*Optical camera system.* An optical-line camera system is used to generate good-quality RGB digital images of the sediment sample surface before the X-ray scan. The line camera incorporates a light-sensitive 2048 pixel CMOS (complementary metal oxide semiconductor) device that has a maximum resolution of 50 μm pixel$^{-1}$. The optical image is available to allow the operator to define the part of the sample to be analysed before scanning, and later serves to relate the radiographic and XRF data to visual colour features of the sediments.

*X-ray source and focusing.* The ITRAX uses a 3 kW X-ray generator and can be used with different tube anodes to obtain excitation for a range of elements. The current system uses a 3 kW molybdenum target tube that can operate up to 60 kV and 50 mA, but the actual voltage–current selected can be optimized for the elements required. In practice 30 kV and 30 mA are suitable for most elements. The X-rays emerging through the shutter of the tube turret are focused by means of a proprietary flat-beam optical device (not a collimator), generating a $20 \times 0.2$ mm rectangular beam with its long axis perpendicular to the sample main axis.

*X-ray line camera.* A digital X-ray line camera is used for recording the intensity of X-radiation transmitted through the sample. The camera, which consists of a linear arrangement of 1024 X-ray sensitive diodes, has a pixel resolution of approximately 20 μm and can operate with exposure times from 20 ms up to several seconds. The images produced by the ITRAX are 'radiographic positives', so that low-density areas appear light and higher density areas appear darker.

## *The XRF detection system*

Reliable XRF analysis requires that the sample–detector distance is kept constant and the ITRAX achieves this by using a laser triangulation system to measure the topography of the sample surface. The XRF detector (Fig. 2), fitted to a vertical motorized stage, adjusts itself according to the topographic scan data previously acquired. The X-ray detector used is a Si-drift detector (SDD). These are proportional solid-state devices that have the advantage of providing high-energy resolution at high count rates but do not require liquid nitrogen cooling, unlike the alternative Si(Li) detectors (Lechner *et al.* 2001). The combination of the SSD, the associated electronics and the digital multi-channel analyser (MCA) allow count rates up to 70 kcps to be handled with only minor degradation in resolution. The SDD operates in a similar manner to a conventional drift chamber. Thus, the electron cloud generated by X-ray quanta absorbed at the surface in the SDD is guided onto a specific readout site on the device. In this way the SDD is analogous to an antenna for X-ray photons. The detector is also fitted with a pumped acrylic nozzle with a thin plastic entrance window to minimize the X-ray attenuation that would otherwise occur with absorption in the air passage between the sample surface and detector.

## *Conventional X-radiography*

Until the advent of digital X-ray cameras, photographic film was used to record images. If the sample is thin and the X-ray source is small enough, each point in the recording device will correspond to a single point in the exposed sample (point-projection radiography). If, however, the source has a finite size there is no longer a simple point-to-point relationship between the recording device and the object. In principle, the structure in the exposed object will be affected by the source size. Structures in the object that are much smaller than the source size will appear blurred in the radiograph, but for structures that are much larger than the source the finite source size will manifest itself in a diffuse zone around the structure termed a penumbra (shadow). The penumbra phenomenon is normally considered to set the ultimate limit of resolution in point-projection radiography. The size of the penumbra is related to the source size and the ratio of the distances (object–camera)/(X-ray source–object). For thick objects, image distortions will also occur because of geometrical aberration generated from rays penetrating the objects far from the optical axis as these rays will penetrate the object off the perpendicular direction. Thus, density gradients that appear perpendicular to the optical axis will only appear sharp in the radiograph close to the optical axis, while further away they will become smoothed out due to this geometrical effect. These phenomena are significant limitations in recording radiographs from extended objects, particularly for objects extending in the same direction as the density gradient to be investigated. This might be the case for cores from trees or sediments where the main interest is to investigate the density variation along the length axis. Another source of distortion for thick objects is from forward-scattered Compton (incoherent) radiation that is also recorded with the transmitted radiation. For

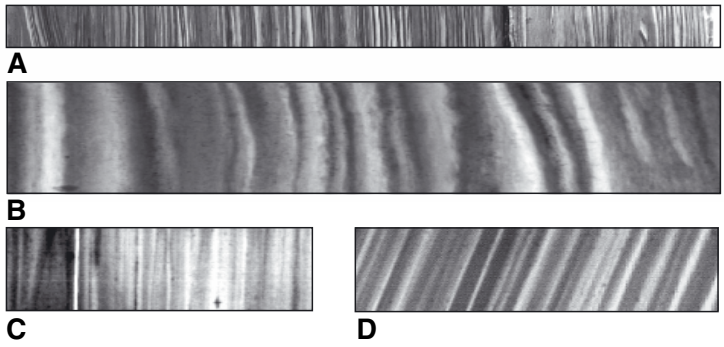


**Fig. 3.** Examples of ITRAX X-radiographic images from a variety of sediments: (**A**) laminated sediment core (200 mm length); (**B**) a 25 mm detail (left of centre) from (A); (**C**) a Moroccan laminite (3 cm in length); and (**D**) North Sea layered sandstone reservoir rock (5 cm in length). All images are 20 mm wide.

thinner objects the problem is less severe as forward Compton scattering is substantially reduced, but the forward Rayleigh (coherent) scattering component will still degrade spatial resolution.

*Benefits of ITRAX flat-beam radiography*. One way to avoid the problems of geometrical aberrations and blurring from scattered radiation is to combine a narrow, parallel, high-flux X-ray beam with an X-ray line camera, and to record the radiograph by moving the object in a regular incremental manner. The use of a high-flux beam allows the line camera to record transmitted signals with relatively short dwell times per increment. The ideal movement direction of the object is parallel to the axis of the density gradient (e.g. perpendicular to sediment layering). Radiographic images are built up by successively adding the recorded radiographic information, line by line, while new areas of the sample move through the beam. By using a narrow (adjustable) slit between the object and the line camera the geometrical aberration and the contribution of scattered radiation can be reduced to practically zero, particularly in the vertical direction. The spatial resolution in the vertical direction is set by the width of the slit in front of the X-ray line camera, and the resolution in the horizontal direction is set by the size of the individual pixels in the diode array.

*ITRAX radiographic resolution*. The resolution and contrast in radiographic images is related to the type of X-ray source used. The 3 kW Mo X-ray tube commonly used produces sufficient energy at 55 kV for transmission through split-core samples of 10 cm diameter. For thinner core samples lower X-ray energies from a Cu or Cr tube could also be used effectively for specific applications. During factory set-up the radiographic resolution and contrast are evaluated using a 1 cm-thick parallel slab of finely laminated sediment, an 11 cm-thick layered sediment and an aluminium block with 15 sharp steps. The resolution is estimated by comparing the sharpness of the intensity rise corresponding to the each step in the aluminium block while the slit width was gradually reduced. When no further increase in sharpness is observed when reducing the slit width, the resolution corresponds to the actual slit size. Resolution is also recorded by estimating the minimum size of significant layers in the radiographs from the two sediment samples while reducing slit width in the same manner described above. The results show that for thin samples the ultimate resolution achievable is about 20 μm, while for approximately 11 cm-diameter split-sediment cores the ultimate resolution is about 100 μm. Some examples of image quality and resolution are shown in Figure 3 for a range of sample types.

## *ITRAX XRF analysis*

XRF elemental detection limits are related to the type of X-ray source used, and the 3 kW Mo tube is well suited for working on split-core samples as it produces good excitation for a range of elements of environmental interest. Enhanced excitation for the lower Z elements may be achieved, at the cost of poorer excitation of the medium Z elements, by using a Cu or Cr tube. However, the regular changing of tubes is preferred to be avoided due to the inconvenience of dismantling and re-instating the water-cooling circuitry. In practice, a single Mo tube is adequate and a good range of elements can be obtained when operating at 30 kV and 30 mA.

### *ITRAX XRF sensitivity*

The sensitivity of the XRF system was evaluated using various international reference samples; United States Geological Survey (USGS) marine sediment MAG-1, USGS manganese nodules NOD-A-1 and NOD-P-1, USGS Green River Shale SGR-1 and US National Institute of Standards and Testing (NIST) Borosilicate Glass 1411. Samples from these materials (except the NIST glass) were prepared as dry, pelletized briquettes and measured on the ITRAX. The detection limits were defined as the elemental concentration corresponding to a peak area equivalent to three times the square root of the average background at the peak position. For a given sample composition, the detection limits vary substantially across the X-ray energy range according to tube anode, tube voltage, count rate and sample composition, as

**Table 2.** *Comparison between ITRAX and conventional WD-XRF*

| | ITRAX | Conventional WD-XRF |
|---|---|---|
| Services required | Three-phase power, water cooling | One- or three-phase power, water cooling |
| Typical X-ray tube used | 3 kW Mo or 2.4 kW Cu | 4 kW Rh |
| High resolution X-radiography provided | Yes | No |
| Optical image provided | Yes | No |
| X-radiographic spatial resolution (selectable) | $\geq$100 μm | Not possible |
| Potential to add other sensors to the scanner | Yes | Unlikely |
| Time to acquire optical image X-radiograph data for a 1 m core at 200 μm resolution | 0.5 h | Not possible |
| Sample treatment and preparation requirement | Non-destructive<br>Flat exposed surface needed<br>6 μm polypropylene film used to inhibit drying during analysis | Semi-destructive (pellets) or destructive (beads)<br>Requires 3 g or more of sample; involves subsample removal, drying, grinding and pelletization |
| Vacuum system required for XRF analysis | Limited option | Yes |
| Helium system option available for volatile or powder samples | No | Yes |
| Practicable scanning resolution | $\geq$100 μm | 5000 μm |
| Time to acquire data for a 1 m core at 200 μm scanning increments for selected elements (K, Ca, Fe, Sr) | 2 h | 10 working days<br>(for 100 sample at 1 cm resolution) |
| Time to acquire data for a 1 m core at 200 μm scanning increments (e.g. Si, Al, K, Ca, Ti, Fe, Mn, Zn, Sr, Zr) | 15 h | 10 working days |
| Time to acquire data for a 1 m core at 200 μm scanning increments (e.g. Si, Al, S, Cl, K, Ca, Fe, As, Pb, Zn, Br, Rb, Sr, Zr) | 48 h | 10 working days |
| Elemental capability for an argillaceous sediment | Si, Al, S, Cl, K, Ca, Ti, Fe, As, Pb, Zn, Br, Rb, Sr, Zr, Ba | Na–U |
| Elemental capability for a carbonate sediment | Cl, Ca, Ba, Fe, Zn, Br, Sr | Na–U |
| Nominal detection limits (100 s); see Table 3<br>Dependent on tube anode, excitation conditions, count-time, atomic number and sample composition | 150 ppm for Ti<br>10 ppm for Sr | 10 ppm for Ti<br>0.5 ppm for Sr |
| General analytical data quality for sediments | Good for elements named above and particularly for fine-grained materials | High for most elements because of highly controlled preparation approach |

is well established in XRF analysis (Jenkins 1999). For indicative purposes the detection limits were recorded with a Mo-anode X-ray tube operating at two different voltages and current, optimized for medium–heavy elements and lighter elements, respectively (Table 2). It is noteworthy that wet and organic-rich sediment material may be associated with poorer detection limits caused by the less efficient excitation of elements because of increased scattering, but grain size and degree of compaction may also affect response.

## Second-generation ITRAX

The prototype ITAX core scanner output all the data as peak area integrals for elements. Further developments allowed quantitation of the count data, and comparison of these integrals with quantitative WD-XRF data (Figs 4 & 6, later) shows that there is a good correlation between the profile shapes obtained with the two techniques – except in some situations where X-ray absorption/enhancement effects become apparent with the ITRAX data. One clear example of this is shown in figure 4 of Thomson *et al.* (2006) where the sapropel layer (S1), which is rich in sea water and organic matter, shows a lower K/Ti than the main trend. This response is an XRF inter-element effect caused by the sea-water chlorine atoms absorbing the potassium K$\alpha$ X-rays. Had the count-rate data been converted to concentrations then the lower K/Ti dip shown should not occur as inter-element corrections would have been applied.

### *XRF elemental sensitivity*

The second-generation ITRAX shows a significant improvement in the overall XRF elemental sensitivity, particularly for Si and above (Table 3). Al sensitivity has also been improved but remains rather imprecise at the present time. The enhancement in response has been achieved by adjusting the orientation of the X-ray capillary optic to allow greater transmission of the primary bremmstrahlung, thereby providing improved excitation to the lower atomic number elements without detriment to the heavier elements. Additional improvements arise from developments with the detector preamplifier and counting electronics that allow higher count rates without significant loss of energy resolution.

**Table 3.** *ITRAX detection limits for ITRAX instruments*

| | ITRAX (Prototype) | ITRAX (Second generation) | Improvement factor |
|---|---|---|---|
| Voltage | 45 kV | 30 kV | |
| Current | 40 mA | 40 mA | |
| Al | not detectable | 22 000 ppm | – |
| Si | 33 000 ppm | 9000 ppm | 4× |
| K | 450 ppm | 150 ppm | 3× |
| Ca | 200 ppm | 100 ppm | 2× |
| Ti | 120 ppm | 60 ppm | 2× |
| Mn | 40 ppm | 25 ppm | 2× |
| Fe | 60 ppm | 25 ppm | 2× |
| Rb | 10 ppm | 5 ppm | 2× |
| Sr | 10 ppm | 5 ppm | 2× |

The data are based on measurements using international geochemical reference samples USGS-MAG1 and USGS-SGR1.
Note that wet sediment may be less efficiently excited owing to less compaction, higher water content and grain-size issues.
Measurement time is 100 s.

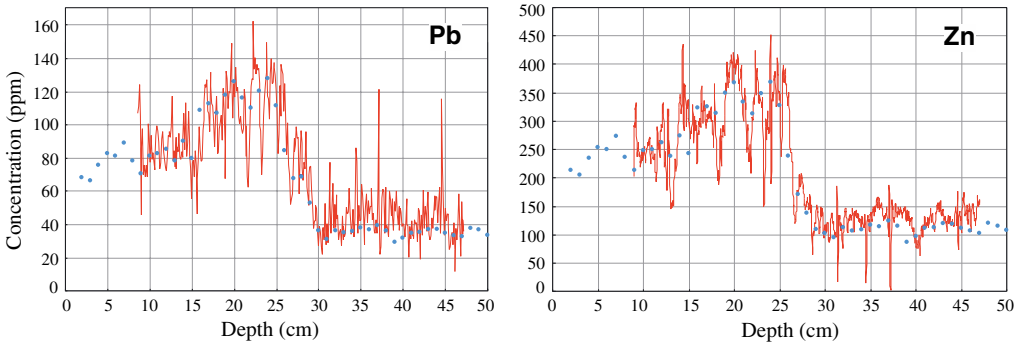


**Fig. 4.** Comparison between WD-XRF and ITRAX (second generation) data for a laminated sediment from the Newport Deep (NPD7), Severn Estuary, UK. The dots represent contiguous samples 1 cm thick analysed using WD-XRF and the continuous red line is the ITRAX profile obtained on the split core.

**Table 4.** *XRF data determined for pelletized USGS reference materials using the ITRAX (second-generation) system*

| | MAG-1 Measured wt% | MAG-1 Recommended wt% | SGR-1 Measured wt% | SGR-1 Recommended wt% |
|---|---|---|---|---|
| $Al_2O_3$ | 16.6 | 16.37 | 5.5 | 6.52 |
| $SiO_2$ | 51.1 | 50.36 | 27.6 | 28.24 |
| $K_2O$ | 5.6 | 3.55 | 2.7 | 1.66 |
| CaO | 1.45 | 1.37 | 8.53 | 8.38 |
| $TiO_2$ | 0.79 | 0.75 | 0.23 | 0.264 |
| MnO | 0.11 | 0.098 | 0.08 | 0.034 |
| $Fe_2O_3$ | 7.23 | 6.8 | 3.09 | 3.03 |
| Ni | 0.005 | 0.0053 | 0.004 | 0.0029 |
| Cu | 0.004 | 0.0030 | 0.0076 | 0.0066 |
| Zn | 0.014 | 0.0130 | 0.0071 | 0.0074 |
| Rb | 0.017 | 0.0149 | 0.0093 | 0.0083 |
| Sr | 0.015 | 0.0146 | 0.043 | 0.042 |

MAG-1, muddy marine sediment with low carbonate content from the Wilkinson Basin, Gulf of Maine.
SGR-1, petroleum and carbonate-rich shale from the Mahogany Zone, Green River Formation.

### *XRF analysis software*

A refined 'XRF fundamental parameters' model is now used in Q-Spec to compensate for inter-element effects and to enable the conversion of count rates to concentration (see Table 4). The user is currently responsible for providing quantification and is able to use suitable reference

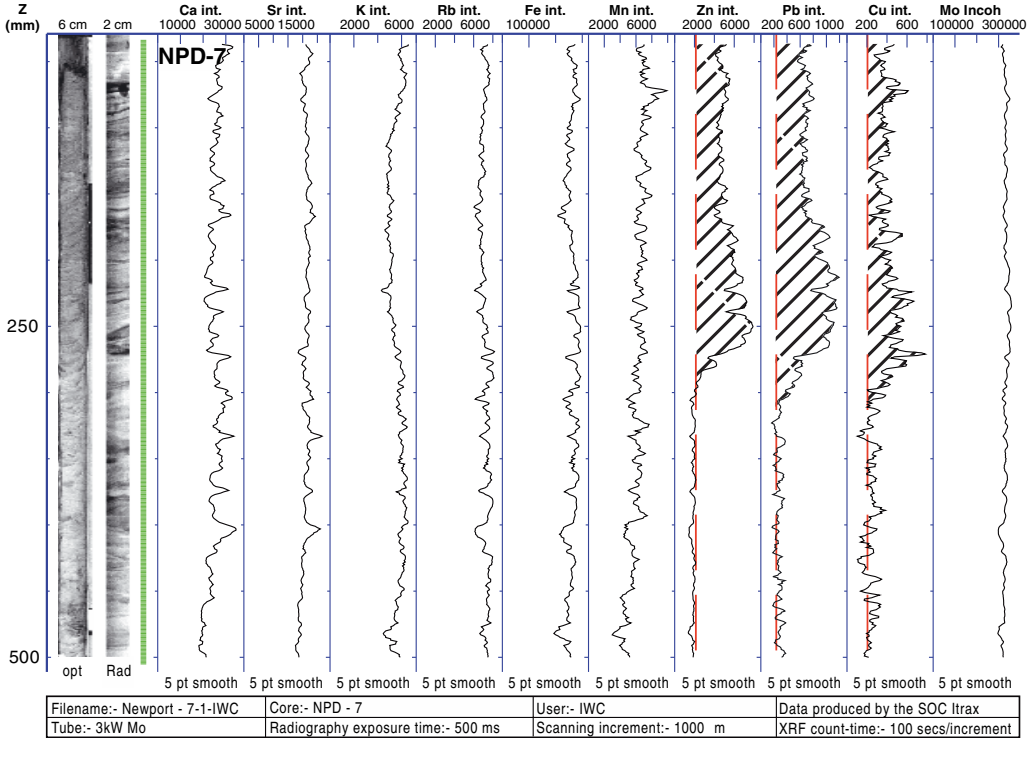


**Fig. 5.** Integrated optical, radiographic and XRF data (Prototype ITRAX) for a laminated sediment core section from the Newport Deep (NPD7), Severn Estuary, UK. Note that levels of the anthropogenic pollutant elements Zn, Pb and Cu are higher in the upper 275 mm. The major elements Ca, K, Fe and Mn and trace elements Sr and Rb show much less variation throughout the core. The green line indicates a valid ITRAX measurement while the red broken lines are user-defined reference lines. Image generated using the program ItraX-Plot.

samples to facilitate this process. This system uses the intensity of the scattered (Compton and Rayleigh) lines from the X-ray tube as a means of normalization, making the quantitative result independent of tube ageing or any other factor affecting the primary beam intensity. The ratio of the Compton and Rayleigh scattered intensities are used to estimate the variation of the average atomic number in the sample.

### *Data visualization software*

The efficient visualization of the analytical data and images from the ITRAX is an important part of the evaluation process, and the National Oceanographic Centre has produced a flexible package called ItraX-Plot for examining and manipulating the core data (see, for example, Figs 5 & 6). The software opens the ITRAX files and allows the user to manipulate, re-size and optimize image files (optical and radiographic), as well as plotting up to 10 XRF elemental profiles at a time. Other options include adjustment of scaling, data smoothing, application of elemental divisors, inclusion of regions of interest, and the addition of horizontal and vertical reference lines. ItraX-Plot also allows temporary removal of suspect or meaningless data prior to final presentation but the original data are never modified. The images can be output or saved in high-quality formats as .PDF, .JPG or .BMP. Cox Analytical also produce an in-house package called RediCore for inspecting and displaying the downcore profiles.

### *Quantification issues in micro-XRF analysis*

The ITRAX geochemical data are normally output as counts and can be considered semi-quantitative in nature, and as such need to be interpreted with caution. Errors may arise due to poor peak discrimination in the X-ray spectra, porosity changes, compaction or grain-size/shape-related artefacts (recorded for K and Sr) and low count rates. Invalid data may be recorded when the X-ray detector is not in the correct position, particularly when the cut core surface is uneven or shows sudden variability from crack-related effects. Careful study of variation in the element integral profiles, the Compton scatter integral and the detector–sediment distance (validity) index can aid in identifying

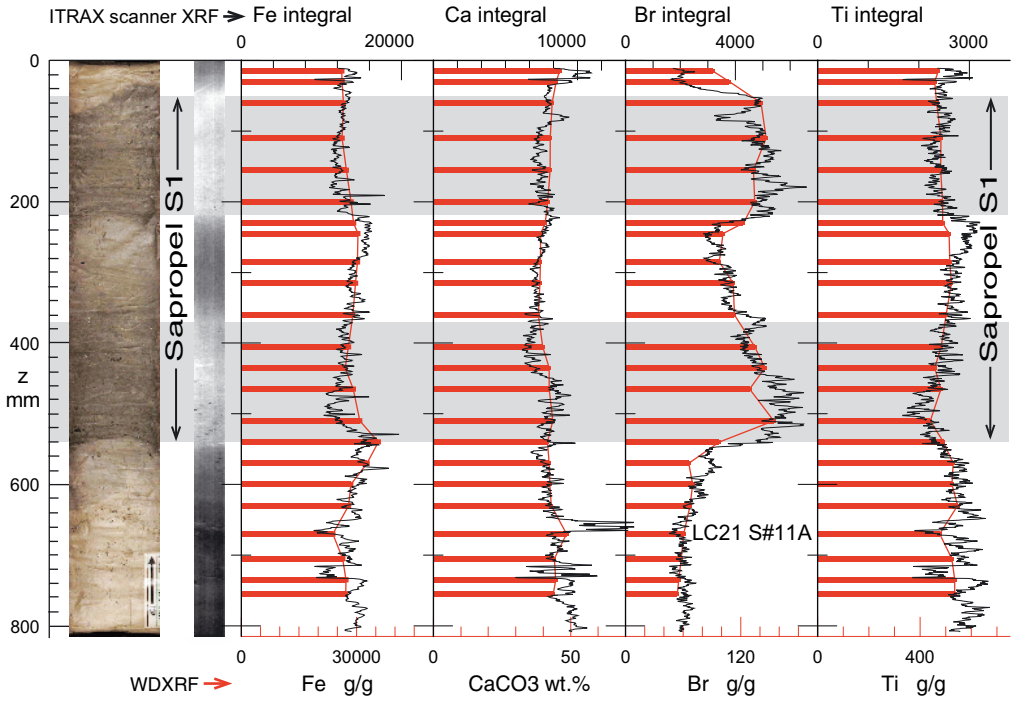


**Fig. 6.** Comparison between WD-XRF data (red bars at 1 cm resolution; scale at bottom) and ITRAX scan elemental integral profiles (Prototype ITRAX; continuous black lines; 200 μm resolution; scale at top) for Mediterranean sediment core (LC21 S#11A) containing the sapropel S1.

such invalid data. The ItraX-Plot data visualization software allows for ready examination of the data at various scales to consider whether they are spurious.

Quantitative ITRAX X-ray microanalysis of natural samples can be successfully carried out, but usually involves a post-processing refinement session followed by a full batch re-analysis. Quantification uses 'XRF fundamental parameters' calculations and assumes compositional and physical homogeneity for the measured samples, and any deviation from this ideal state will introduce errors. The effectiveness of the quantitation will be impaired for some sample types where the small excitation volume, medium–coarse grain sizes and mineral effects combine. The analysis of natural samples containing discrete medium–coarse fragments (e.g. quartz, feldspar, rutile, ilmenite, zircon, biogenic carbonate clasts) may lead to analytical inaccuracies and will be most significant when measuring low Z elements or low energy X-ray energies. Where the unknown and reference samples have similar granular structures and elemental and mineral compositions then these problems can be reduced. Another effect requiring consideration is where pore-water solutes can dry out on a sediment surface, which will lead to spurious count rates. Frequently, this effect can be remedied by careful removal of a thin surface layer (using a glass slide, for example) prior to analysis. In spite of the potential problems noted above, the elemental profiles obtained using the ITRAX show that useful semi-quantitative and quantitative data can be obtained for a good range of elements.

### *ITRAX measurement accuracy and precison*

The analytical data shown in Figure 4 and Table 4 demonstrate that reasonable accuracy can be achieved. The poorer $K_2O$ data (Table 4) found when quantifying XRF data for the USGS reference samples may reflect unresolved inter-element or particle-size effects. The next stage in the development of the ITRAX system is to develop and refine the conversion of count data to concentration data.

The measurement precision of the ITRAX can be simply determined by calculating the square root of the count integral. Another means of estimating precision is from the general smoothness or spikiness of the XRF elemental profiles (e.g. Figs 4–6). Some variations reflect statistical noise or changes caused by compositional boundaries or cracks.

## Examples of ITRAX applications

The capability of the ITRAX core scanner has been evaluated by investigating diverse sediment types from wet, unconsolidated materials such as cores from the eastern Mediterranean Sea containing sapropels (Thomson *et al.* 2006) to heavy metal-polluted estuarine sediment. Other sample types such as peat, organic-rich lake sediment and mineralized rocks have also been examined. Some of the compositional parameters that can aid in routine sedimentological or lithostratigraphic analysis of marine sediment cores are summarized in Table 5. Further details of such information can be found in Rothwell *et al.* (2006) and Thomson *et al.* (2006). Two specific examples of ITRAX applications are given here.

### *Polluted Severn Estuary sediment*

A subtidal sediment core collected from the Newport Deep, Severn Estuary (Fig. 5) was investigated to examine records of metal pollution from different industrial sources. Earlier studies by Allen & Rae (1986) and Allen (1988) had defined chemozones in sediment cores from the Severn Estuary. A recent study by the first author examined sedimentological, radiometric and geochemical data from the Newport Deep to determine the record of anthropogenic inputs in several sediment cores. The ITRAX was used to compare elemental profiles with those obtained using a Philips MAGIX-Pro WD-XRF spectrometer, also based at the National Oceanography Centre, Southampton. The latter method, though delivering high-quality quantitative data, involved subsample collection and took approximately 8–10 days overall to acquire the final data. By contrast, ITRAX analysis only involves halving the core followed by measurement, which may take approximately 2 days if trace-element data are required (1 m core scanned at 200 μm resolution with an XRF measurement time of 100 s per increment).

The ITRAX radiographs acquired for Newport Deep sediment cores NPD7 (Fig. 5) show distinctive mm-scale layering caused through variations in carbonate, clay and sand. Some elemental profiles show steps, very similar to those previously seen using the Philips WD-XRF. These steps are clearly evident for Cu, Zn and Pb in the ITRAX profiles (but are also evident for a wider set of elements with the WD-XRF, i.e. P, Cr, As, Sn, I and S) and are caused by anthropogenic inputs of heavy metals to the estuary over the last 50 years or more. Additional

**Table 5.** *Examples of ITRAX output parameters that aid in sedimentological or lithostratigraphic analysis*

| Property measured | ITRAX detection efficiency | Comment on property |
|---|---|---|
| Compton scattering $MoK_{inc}$ | High | • Relates inversely to the mean atomic number<br>• Will vary with mineralogical composition, water and organic carbon content<br>• Inflections may occur at bed boundaries<br>• Will vary with sediment packing density |
| Ca/Fe | High | • Indicative of biogenic carbonate : detrital clay ratio<br>• May show strong correlation with sedimentary units<br>• Ca/Fe profile is a good proxy for sediment grading and for assessing source relationships<br>• Can distinguish foraminifer- or shell-rich layers |
| Sr/Ca | High | • Enhanced Sr may indicate the presence of high-Sr aragonite which requires a shallow-water source<br>• Affected by sediment packing/porosity and grain-size/shape variations |
| K/Rb | Moderate | • K is commonly associated with detrital clay and may be enhanced in turbidite muds<br>• Potentially unreliable parameter as sea-water Cl atoms will absorb potassium X-rays, so apparent high K may reflect increased porosity |
| Zr/Rb<br>Ti/Rb | Moderate | • Zr and Ti are high in heavy resistate minerals and may be enhanced in turbidite bases<br>• Useful as sediment-source/provenance indicators |
| Si | Moderate–low | • Important terrigenous or productivity indicator<br>• Normalization using detrital divisor can distinguish terrigenous or productivity origin<br>• May be useful as a sediment-source and provenance indicator |
| Fe/Rb<br>Fe/Ti | Good | • Commonly shows grain-size-related fractionation effects<br>• Fe mobilized during redox-related diagenesis and elevated Fe commonly seen in oxic, or formerly oxic, parts of sediment<br>• Rb is an element commonly associated with detrital clay and may be enhanced in turbidite muds |
| Cu/Rb<br>Cu/Ti | Moderate | • Sharp Cu peaks are largely of diagenetic origin |
| As | Moderate | • Commonly an indicator of pyrite which may be detrital or authigenic in origin |
| Mn/Ti | Good | • Good indicator of redox-related diagenesis |
| Ba/Ti | Low–moderate | • Important productivity indicator |
| Br/Cl<br>S/Cl | Moderate–low | • For marine sediments a constant ratio implies sea-water ratios. High ratios may indicate organic-rich layers as Br and S are high in organic-rich sediments |

The property refers to an element ratio or peak area integral.
See Rothwell *et al*. (2006) and Thomson *et al*. (2006) for more specific discussion of the above parameters.

cores examined from the Severn Estuary confirm the findings seen in NPD7.

### *Mediterranean sediment with sapropel*

A well-characterized subcore held in the BOSCORF archive (Section 11A of core LC21), previously examined by Mercone *et al*. (2000, 2001), was scanned (Fig. 6). This core contains an example of the organic-rich sedimentary units (sapropels) that form periodically in the eastern Mediterranean basin. Sapropels are visually distinct because of their dark colour, but the ITRAX X-radiograph also reveals coincident physical property changes that result mainly from the lower sediment density and

high pore-water content in sapropels. ITRAX elemental profiles were compared with wavelength dispersive XRF data from discrete 1 cm samples taken through the most recent sapropel (S1). While recognizing that the measured XRF element integrals from the ITRAX do not have an exact constant relationship with element concentration over changing sediment types, the data show a good comparison (Fig. 6). There are plans to quantify the ITRAX data routinely. The ITRAX data (discussed in detail by Thomson *et al.* 2006) show that higher Ba/Ti and Br/Cl ratios correspond with the high $C_{org}$ content in the visual and oxidized sapropel. The thinning of the original sapropel thickness by post-depositional oxidation is revealed from Mn/Ti and Cu/Ti ratios, pyrite authigenesis in the residual visual sapropel from Fe/Ti and S/Cl ratios and the As integral, and aragonite formation in and around the sapropel from the Sr/Ca ratio.

## Conclusions

The ITRAX multi-function core scanner has the capability to rapidly and conveniently acquire data for three important physical and chemical properties from split-sediment cores. A scanner run will provide a high-quality optical image file, a 16-bit X-radiography image file and multiple X-ray spectral files, and an immediate end-of-run analytical summary. Further post-run re-processing of X-ray is straightforward. This combined acquisition of physical and chemical data is of considerable attraction where initial non-destructive characterization of lake and marine sediment and rock cores is required. The ITRAX may be an acceptable substitute for traditional analytical methods in some cases and for some elements, but more generally it will be useful in acquiring indicative data for cores held in repositories before destructive sampling for further detailed investigations. XRF scanner systems cannot be expected to deliver a quality of data comparable to that of systems such as WD-XRFs because of the small excitation volume used, the air path, and the effects of mineralogy, particle size, porosity and water content variations. Their high-resolution capability, however, considerably exceeds that achievable by conventional sampling methods and may lead to specific new applications (e.g. ombrotrophic peat analysis, examination of mineralized rock sections). The ITRAX instrument also provides a convenient platform for adding other sensors (e.g. Fourier Transform Infra Red spectroscopy, spectrophotometry) that may provide helpful data such as have been used to extract palaeoenvironmental information from cores (Giosan *et al.* 2002*a*,*b*; Berg & Jarrard 2003).

I.W. Croudace and R.G. Rothwell, and other colleagues and former colleagues at NOC, particularly Professors C. German, J. Thomson and P. Weaver, are grateful to the UK Office of Science and Technology via the Natural Environment Research Council for providing funds to purchase X-ray analytical instruments that included the ITRAX. The realization of the ITRAX core scanner is due to a co-operative venture between COX Analytical (A. Rindby, B. Stocklasser, P. Engstrom, S. Norder and J. Rudolfsson) and NOC (I.W. Croudace and R.G. Rothwell). We thank NOC colleagues R. Pearce for the loan of laminated sediment blocks and K. Davis for improvements to the technical artwork.

## References

Allen, J.R.L. 1988. Modern-period muddy sediments in the Severn Estuary (southwestern UK): a pollutant-based model for dating and correlation. *Sedimentary Geology*, **58**, 1–21.

Allen, J.R.L. & Rae, J.E. 1986. Time sequence of metal pollution, Severn estuary, southwestern UK. *Marine Pollution Bulletin*, **17**, 427–431.

Berg, M.D.V. & Jarrard, R.D. 2004. Cenozoic mass accumulation rates in the equatorial Pacific based on high-resolution mineralogy of Ocean Drilling Program Leg 199. *Paleoceanography*, **19**, 1–12. PA2021, doi: 10.1029/2003PA000928.

Bergström, U., Lindeberg, J. & Rindby, A. 2001. Batch measurements of wood density on intact or prepared drill cores using X-ray microdensitometry. *Wood Science and Technology*, **35**, 435–452.

Croudace, I.W. & Williams-Thorpe, O. 1988. A low dilution, wavelength-dispersive X-ray fluorescence procedure for the analysis of archaeological rock artefacts. *Archaeometry*, **30**, 227–236.

Croudace, I.W. & Gilligan, J. 1990. Versatile and accurate trace element determinations in iron-rich and other geological samples using X-ray fluorescence analysis. *X-ray Spectrometry*, **19**, 117–123.

Giosan, L., Flood, R.D. & Aller, R.C. 2002*a*. Paleoceanographic significance of sediment color on western North Atlantic drifts: I. Origin of color. *Marine Geology*, **189**, 25–41.

Giosan, L., Flood, R.D., Grutzner, J. & Mudie, P. 2002*b*. Paleoceanographic significance of sediment color on western North Atlantic Drifts: II. Late Pliocene-Pleistocene sedimentation. *Marine Geology*, **189**, 43–61.

Jansen, J.H.F., Van der Gaast, S.J., Koster, B. & Vaars, A.J. 1998. CORTEX, a shipboard XRF-scanner for element analyses in split sediment cores. *Marine Geology*, **151**, 143–153.

Janssens, K., Adams, F. & Rindby, A. (eds). 2000. *Microscopic X-Ray Fluorescence Analysis*. Wiley, Chichester.

JENKINS, R. 1999. *X-Ray Fluorescence Spectrometry*, 2nd edn. Wiley, Chichester.

LECHNER, P., FIORINI, C. *ET AL.* 2001. Silicon drift detectors for high count rate X-ray spectroscopy at room temperature. *Nuclear Instruments and Methods*, **458A**, 281–287.

MERCONE, D., THOMSON, J., ABU-ZIED, R.H., CROUDACE, I.W. & ROHLING, E. 2001. High-resolution geochemical and micropalaeontological profiling of the most recent eastern Mediterranean sapropel. *Marine Geology*, **177**, 25–44.

MERCONE, D., THOMSON, J., CROUDACE, I.W., SIANI, G., PATERNE, M. & TROELSTRA, S.R. 2000. Duration of S1, the most recent eastern Mediterranean sapropel as indicated by AMS radiocarbon and geochemical evidence. *Palaeoceanography*, **15**, 336–347.

RINDBY, A., ENGSTRÖM, P. & JANSSENS, K. 1997. The use of a scanning X-ray microprobe for simultaneous XRF/XRD studies of fly-ash particles. *Journal of Synchrotron Radiation*, **4**, 228–235.

ROTHWELL, R.G., HOOGAKKER, B., THOMSON, J., CROUDACE, I.W. & FRENZ, M. 2006. Turbidite emplacement on the southern Balearic Abyssal Plain (western Mediterranean Sea) during Marine Isotope Stages 1–3: an application of ITRAX XRF scanning of sediment cores in lithostratigraphic analysis. *In*: ROTHWELL, R.G. (ed.) *New Techniques in Sediment Core Analysis*. Geological Society, London, Special Publications, **267**, 79–98.

STRELI, C., WOBRAUSCHEK, P., PEPPONI, G. & ZOEGER, N. 2004. A new total reflection X-ray fluorescence vacuum chamber with sample changer analysis using a silicon drift detector for chemical analysis. *Spectrochimica Acta*, **B59**, 199–203.

THOMSON, J., CROUDACE, I.W. & ROTHWELL, R.G. 2006. A geochemical application of the ITRAX scanner to a sediment core containing eastern Mediterranean sapropel units. *In*: ROTHWELL, R.G. (ed.) *New Techniques in Sediment Core Analysis*. Geological Society, London, Special Publications, **267**, 65–77.

TSUJI, K., INJUK, J. & VAN GRIEKEN, R. (eds). 2004. *X-ray Spectrometry: Recent Technological Advances*. Wiley, Chichester.

VINCZE, L., JANSSENS, K., ADAMS, F., RINDBY, A. & ENGSTRÖM, P. 1998. Interpretation of capillary generated spatial and angular distributions of X-rays: theoretical modelling and experimental verification using the European Synchrotron Radiation Facility Optical beam line. *Review of Scientific Instruments*, **69**, 3494–3503.